DOI: 10.1002/ejic.200900152

A New 5,5′-Bitetrazole Thorium(IV) Compound: Synthesis, Crystal Structure and Quantum Chemical Investigation

Roland W. H. Pohl,[a] Jonas Wiebke,[b] Axel Klein,*[a] Michael Dolg,[b] and Nicola Maggiarosa[a][‡]

Keywords: Actinides / Bitetrazole / Hydrates / Thorium / X-ray diffraction / Density functional calculations

Thorium(IV) 5,5′-bitetrazolate hydrate $C_4H_{26}N_{16}O_{13}Th$ has been prepared and structurally analysed by single crystal XRD. The compound crystallises in the triclinic space group $P\bar{1}$ with the cell constants a = 1058.2(2), b = 1081.6(2), c = 1136.7(2) pm, α = 73.46(2), β = 83.98(2), γ = 66.01(2)°. The observed structure is similar to the salt-like structures of the corresponding Tb^{III} and Er^{III} systems with respect to the non-coordinating behaviour of the 5,5′-bitetrazolate dianions. The Th^{IV} cations form discrete hydroxo-bridged binuclear thorium-aqua complexes with Th–Th distances of 399(7) pm. Comparison with structural data of known hydrolysis products of the hydrated Th^{IV} cation, and density functional calculations on gas phase molecular clusters, employing relativistic *large-core* pseudopotentials and large *valence-only* (7s7p5d2f1g)/[6s5p4d2f1g] basis sets for Th^{IV}, confirm the identification of the cation in $C_4H_{26}N_{16}O_{13}Th$ as $[(\mu\text{-}OH)_2\text{-}Th_2(H_2O)_{14}]^{6+}$.

Introduction

In his Nobel lecture in 1922, Niels Bohr predicted a series of 5*f* elements, although he did not specify the element from which the series would start. Later on, Seaborg discovered that the 5*f* series starts from actinium and is the "second rare-earth series".[1] Concepts emphasising the similarity of actinides to *d*-elements were suggested by Zachariasen[2] and Haissinsky.[3] Choppin's 1995 review[4] began with the statement that the concept advanced by Seaborg, regarding the close chemical similarity between trivalent lanthanides and actinides, is frequently presented as the main success of the periodic system and finished with a conclusion as to the exact likeness in thermodynamic properties of the 4*f* and 5*f* elements. The primal difference between lanthanides and actinides is the existence of stable high oxidation states of the lighter actinides. In contrast, high lanthanide oxidation states, e.g. Ln^{V} or Ln^{VI}, are spoiled by the strongly localised nature of the 4*f* (as compared to the 5*f*) orbitals, which is a consequence of both the absence of orthogonality constraints with respect to inner shells of the same angular symmetry, and to a smaller impact of relativistic effects.[5] Till this day the discussion is vivid whether Th^{IV} has to be considered as an actinide element or as a large member of the group IV elements, with recent contributions on the chemistry of the complexes $[(Cp^*)_2M(Me)_2]$ (M = Zr, Hf, Th),[6] on quantum chemical calculations on the Cp derivatives $[(Cp)_2M(Me)_2]$ (M = Zr, Th, U),[7] or on spectroscopic similarities and differences.[8]

Recently, our group reported on the 5,5′-bitetrazole coordination chemistry of a number of trivalent 4*f* element ions.[9] Generally, the 5,5′-bitetrazolate dianion BT^{2-}[10–12] and related tetrazolyl systems are interesting candidates for rich coordination chemistry: For example, BT^{2-} contains eight N atoms, being able to act as mono-, bi-, tri- or tetradentate ligand (cf. Scheme 1), and might therefore give rise to mononuclear, binuclear, or oligonuclear complexes (coordination polymers), as well as the formation of one-, two-, or three-dimensional networks in the solid state.

Particularly, BT^{2-} has been found to employ both η^2 and $\mu,\eta^1{:}\eta^1$ coordination modi in $[Ln_2(BT)_3]\cdot 14H_2O$ for La^{III} and Ce^{III}, and η^2 coordination in $[Ln(BT)(H_2O)_7]_2[BT]\cdot xH_2O$ for Nd^{III}, Sm^{III}, and Eu^{III}, whereas no direct BT–Ln^{III} interaction has been observed in the salt-like Tb^{III} and Er^{III} systems $[Ln(H_2O)_9]_2[BT]_3\cdot H_2O$.[9] This has been attributed to the decrease of Ln^{III} ionic radii, and the increase of Ln^{III} Lewis acid hardness across the series, which effectively favours the H_2O with respect to the BT^{2-} ligands in the competition for the Ln^{III} ions inner coordination shell as one goes from La^{III} to Er^{III}.[9] Considering the overall similarity of the trivalent lanthanide ions and their solution chemistry, it is apparent that the actual BT^{2-} coordination

[a] Universität zu Köln, Institut für Anorganische Chemie, Greinstrasse 6, 50939 Köln, Germany
E-mail: axel.klein@uni-koeln.de
[b] Universität zu Köln, Institut für Theoretische Chemie, Greinstrasse 4, 50939 Köln, Germany
E-mail: m.dolg@uni-koeln.de
[‡] Present address: LG Chem., Ltd., Research Park, Chemicals and Polymers R&D
104-1 Moonji-dong, Yuseong-gu, Daejeon, 305-380, Korea
E-mail: maggnico@lgchem.com

Supporting information for this article is available on the WWW under http://dx.doi.org/10.1002/ejic.200900152 or from the author.

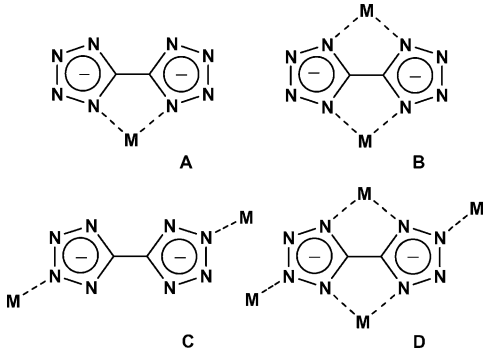

Scheme 1. Feasible coordination modes of BT^{2-}. **A**: chelate η^2; **B**: chelate bridging $\mu,\eta^2:\eta^2$; **C**: monodentate bridging $\mu,\eta^1:\eta^1$ and **D**: mono- and bidentate bridging.

mode, at least in aqueous solution systems, is easy to modulate by comparably slight variations among the metal ions considered. Therefore, and from the primal analogies among lanthanides and actinides, i.e. the 4*f* and 5*f* metals, the BT^{2-} coordination behaviour in similar actinide systems is of general interest.

Recent studies by Soderholm et al. have shown that Th^{IV} coordinates to hard donor ligands as H_2O, Cl^- and nitrate (η^2-O,O) in binuclear hydroxy-bridged complexes,[13] from aqueous solution, in contrast to the softer Br^-, which is not coordinated in $[Th(H_2O)_{10}]Br_4$.[14]

Here we report on the preparation and the crystal structure of the new Th^{IV} BT compound $[(\mu\text{-}OH)_2Th_2(OH_2)_{14}][BT]_4\cdot 10H_2O$, obtained from Th^{IV} nitrate hydrate and sodium 5,5′-bitetrazolate, together with the quantum chemical investigation of some of its structural aspects. We thus extend the range of metal ions considered so far[9] at its "small and hard" side, while providing data on the first bitetrazolate containing compound of a tetravalent metal ion.

Results and Discussion

Preparation and X-ray Diffraction Study

From a mixture of Th^{IV} nitrate hydrate and sodium 5,5′-bitetrazolate dissolved in water we obtained colourless crystals which were submitted to an X-ray diffraction study. Further characterisation was not attempted. The crystal structure was solved in the triclinic space group $P\bar{1}$ and was refined with the results summarised in Table 3.

Single-Crystal Structure

The crystal structure (Figure 1) of the Th^{IV} BT compound reveals discrete binuclear Th_2O_{16} moieties within a one-dimensional network of π-stacked BT^{2-} anions, and a number of intercalated H_2O molecules. The Th_2O_{16} unit is formed from two edge-sharing ThO_9 polyhedra (Figure 2). The shortest Th–O distances of 238(3) and 235(5) pm create a Th_2O_2 parallelogram with O–Th–O and Th–O–Th angles of 65.3(2)° and 114.7(3)°, respectively; the Th–Th distance is 399(7) pm. These data compare well with a number of dimeric Th^{IV} hydrolysis products[13] (Table 1) and suggest the identification of the Th_2O_{16} moiety as $[(\mu\text{-}OH)_2Th_2(OH_2)_{14}]^{6+}$. However, the crystal structure had to be refined without localising the protons. The difficulty to locate low-scattering atoms like protons near heavier atoms is well-known.[15] It is nevertheless justified to presume hydrogen bridges, as found in the corresponding Ln^{III} compounds.[9]

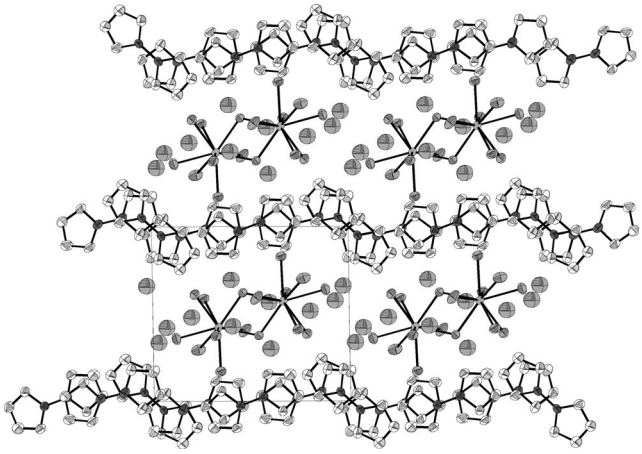

Figure 1. Packing of the $Th^{IV}BT_2$ hydrate. View along the b-axis.

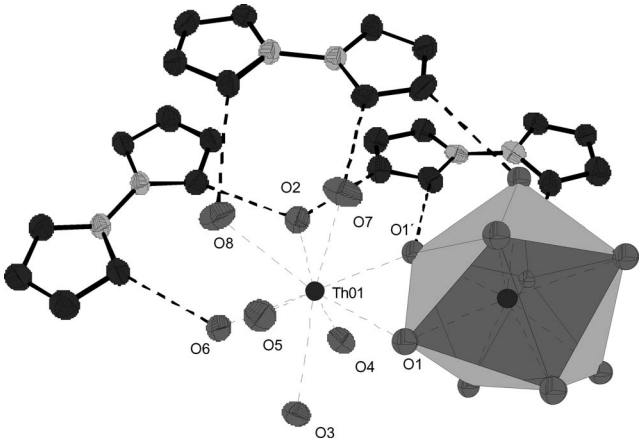

Figure 2. Structure of the $[(\mu\text{-}OH)_2Th_2(H_2O)_{14}]^{6+}$ cation and hydrogen bridges to the anions in the second coordination sphere; ellipsoids presented at 50% probability.

Generally, the finding of discrete Th_2O_{16} moieties with absent Th^{IV}–BT contacts is in line with the recent observation of the coordination behaviour of BT^{2-} in the analogue Tb^{III} and Er^{III} systems:[12] Tb^{III}, Er^{III}, and Th^{IV} have – in a ninefold-coordinated scenario – comparable ionic radii of 109, 106, and 109 pm,[16] respectively, and must be regarded as strong and hard Lewis acids, thus favouring H_2O over BT^{2-} coordination. However, the Th^{IV} system differs in its binuclear Th_2O_{16} motif from the mononuclear $[Ln(H_2O)_9]^{3+}$ units in the Tb^{III} and Er^{III} systems.[9] From the higher positive charge on Th^{IV} it appears natural that, in going beyond the Ln^{III} series, one finds a salt-like Th^{IV}–BT

Table 1. Bond lengths [pm] compared to other dimeric hydroxo-aqua-thorium complexes.

	$[(\mu\text{-}OH)_2Th_2(H_2O)_{14}]^{6+}$[a]	$[(\mu\text{-}OH)_2Th_2Cl_2(H_2O)_{12}]^{4+}$[b]	$[(\mu\text{-}OH)_2Th_2(NO_3)_4(H_2O)_8]^{2+}$[b]
Th–O1	235(5)	235.1(4)	233.3(3)
Th–O1′	238(3)	236.0(4)	236.9(3)
Th–O2	248(2)	249.7(5)	248.2(3)
Th–O3	253(4)	249.4(5)	254.4(3)
Th–O4	250(1)	249.8(5)	248.5(3)
Th–O5	248(3)	252.3(4)	252.1(3)
Th–O6	248(2)	255.4(4)	
Th–O7	252(2)	250.0(5)	
Th–O8	257(4)		

[a] This work. [b] From ref.[13]

compound differing qualitatively in the metal–aquo unit due to its higher Brønstedt acidity – whereas the BT^{2-} dianion's coordination behaviour is as found in the Tb^{III} and Er^{III} systems.

Calculations

To clarify the nature of the Th_2O_{16} subsystem present in the experimental X-ray crystal structure of $C_4H_{26}N_{16}O_{13}Th$, C_i-symmetric $[(\mu\text{-}OH_2)_2Th_2(OH_2)_{14}]^{8+}$ and $[(\mu\text{-}OH)_2Th_2(OH_2)_{14}]^{6+}$ initial molecular structures were constructed by naively adding H atoms to the experimental Th_2O_{16} coordinates, and optimised within C_i symmetry constraints.

The $[(\mu\text{-}OH_2)_2Th_2(OH_2)_{14}]^{8+}$ system optimises to two strongly repelling $[Th(OH_2)_7]^{4+}$ fragments and two separated H_2O molecules. Relaxing the C_i constraints, departing from the same initial structure leads to one $[Th(OH_2)_7]^{4+}$, one H_2O, and one $[Th(OH_2)_6OH{\cdot}OH_3]^{3+}$ fragment similar to the $[Th(OH_2)_7]^{4+}$ fragment. Fixing the Th–Th distance to the experimental value and optimising all other structure parameters within C_i constraints leads to a $[(\mu\text{-}OH_2)_4Th_2(OH_2)_{12}]^{8+}$ system with a central $Th_2(\mu\text{-}O)_4$ distorted octahedral feature, but a large residual gradient norm of 0.12 a.u. Whereas non-central Th–OH_2 distances compare well with experimental data, Th–μ-OH_2 distances $d_{Th1–O1}$, $d_{Th1–O1a}$, $d_{Th1–O7}$, and $d_{Th2–O7}$ miss their experimental counterparts by 42, 39, 21, and 109 pm, respectively (Table 2), i.e. by much more than can be expected from the $[Th(\eta^1\text{-}C_5O_5)_2(OH_2)_7]$ benchmark calculations (see Supporting Information). The situation is similar for $\theta_{O1–Th1–O1a}$ and $\theta_{Th1–O1–Th2}$, missing their experimental counterparts by 22.4 and 22.4°, respectively. Allowing $d_{Th–Th}$ to relax, a subsequent structure optimisation of the $[(\mu\text{-}OH_2)_4Th_2(OH_2)_{12}]^{8+}$ system leads to two $[Th(OH_2)_7]^{4+}$ fragments and two separated H_2O molecules again.

In contrast, the $[(\mu\text{-}OH)_2Th_2(OH_2)_{14}]^{6+}$ system optimises, both with and without C_i constraints, to a cluster structure (Figure 3) that is found to agree reasonably with experimental structure data (Table 2). In $[(\mu\text{-}OH)_2Th_2(OH_2)_{14}]^{6+}$, $d_{Th1–Th2}$ = 427.9 pm overestimates the experimental Th–Th distance of 399.3 pm by 28.6 pm. Accordingly, calculated Th–μ-OH distances $d_{Th1–O1}$ and $d_{Th1–O1a}$ come out too large by 10 and 7 pm as compared to 235 ± 5 and 238 ± 3 pm, respectively. The angular parameters of the central $[Th_2(\mu\text{-}OH)_2]$ unit, i.e. $\theta_{O1–Th1–O1a}$ and $\theta_{Th1–O1–Th2}$, are reasonably close to their experimental counterparts. The H atoms of the μ-OH groups are found to point out of the $[Th_2(\mu\text{-}OH)_2]$ plane by $\theta_{Th1–Th2–O1–H11}$ = 168.15° in a C_i-symmetric fashion; $d_{O1–H11}$ = 97.1 pm. Generally, aqua ligand O–H distances range from 97.2 to 97.8 pm, averaging at 97.6 pm. Gas-phase $[(\mu\text{-}OH)_2Th_2(OH_2)_{14}]^{6+}$ bonding energies are 1769 kJ mol^{-1} with respect to dissociation to independent $[Th(OH_2)_7OH]^{3+}$ fragments, or 8496 kJ mol^{-1} with respect to total decomposition to independent Th^{4+} ions, OH_2, and OH^- fragments.

Table 2. Calculated bond lenghts [pm] and angles [°] compared to experimentally obtained values.

	$[(\mu\text{-}OH_2)_4Th_2(H_2O)_{12}]^{8+}$ [a]	$[(\mu\text{-}OH)_2Th_2(H_2O)_{14}]^{6+}$	Experimental
$d_{Th1–O1}$	276.2	245.1	235(5)
$d_{Th1–O1'}$	276.6	245.1	238(3)
$d_{Th1–O2}$	250.7	252.2	248(2)
$d_{Th1–O3}$	252.0	254.6	253(4)
$d_{Th1–O4}$	251.8	250.3	250(1)
$d_{Th1–O5}$	252.4	255.1	248(3)
$d_{Th1–O6}$	244.8	263.0	248(3)
$d_{Th1–O7}$	273.1	256.1	252(2)
$d_{Th1–O8}$	255.8	259.9	257(4)
$d_{Th1–Th2}$	399.3[a]	427.9	399(1)
$d_{Th2–O8}$	298.4	465.9	441(1)
$\theta_{O1–Th1–O1'}$	87.7	58.37	65(1)
$\theta_{Th1–O1–Th2}$	92.3	121.63	115(1)
$\theta_{Th1–Th2–O1–H11}$	123.4, 115.9	167.82	–

[a] For fixed $d_{Th–Th}$ = 399.3 pm as discussed in the text.

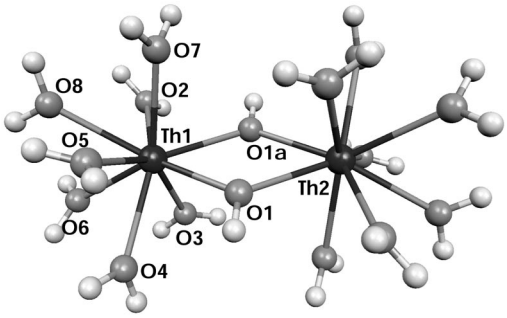

Figure 3. Calculated structure of the $[(\mu\text{-}OH)_2Th_2(H_2O)_{14}]^{6+}$ cation.

Concluding, the aquo-bridged $[(\mu\text{-}OH_2)_2Th_2(OH_2)_{14}]^{8+}$ is not stable with respect to decomposition for gas-phase conditions, whereas the hydroxido-briged $[(\mu\text{-}OH)_2Th_2(OH_2)_{14}]^{6+}$ is at the TPSSh DFT level of theory. If the Th–Th distance is fixed in the aquo-bridged system, its central unit's Th–μ-O distances differ significantly from the Th–μ-O distances of the hydroxido-bridged system's central unit. These, in turn, compare reasonably with experimental structure data. Therefore, within our molecular cluster model, which clearly is limited to qualitative considerations only, we feel safe to conclude that our calculations support the identification of the Th_2O_{16} subsystem in $C_4H_{26}N_{16}O_{13}Th$ with the formula $[(\mu\text{-}OH)_2Th_2(OH_2)_{14}]^{6+}$.

Conclusions

The first bitetrazolate coordination compound of Th^{IV} has been prepared and structurally characterised by means of XRD and, in terms of some of it's structural aspects, by quantum chemical first-principle calculations. $C_4H_{26}N_{16}O_{13}Th$ reveals a salt-like triclinic $P\bar{1}$ structure that does not involve any metal–BT contacts. This is in line with the general trend recently observed for the BT^{2-} coordination behaviour in the analog Ln^{III} systems.[9] In contrast to these, from comparison with structural data of dimeric Th^{IV} hydrolysis products[13] and DFT calculations on simple gas-phase cluster models, $C_4H_{26}N_{16}O_{13}Th$ is found to be best described as formed from discrete binuclear $[(\mu\text{-}OH)_2Th_2(H_2O)_{14}]^{6+}$ moieties within a one-dimensional network of π-stacked BT^{2-} dianions. This complements our recent investigation of the analog rare-earth–BT systems in that, if one goes through and beyond the Ln^{III} series of cations, for a complete picture one needs to consider qualitative changes in the coordination behaviour of both BT^{2-} and the metal cation, including hydrolysis of the metal–aqua moieties.

Experimental Section

General Remarks: Radioactive material, even though natural thorium shows only alpha decay, should be handled with extreme care. Therefore all manipulations with thorium salts were performed in a glovebox. Due to the explosive nature of nitrogen-rich materials, safety equipment like leather gloves, face-shield and ear protection are strongly recommended. All NMR spectra were recorded from concentrated (approximately 6 M) solutions in D_2O at ambient temperature on a Bruker Avance 400 MHz spectrometer; data are given in ppm. Elemental analyses were performed using a HEKAtech Euro EA 3000 analyser. High resolution negative ESI-MS spectra were measured on a Finnigan 900 S spectrometer equipped with a double focusing sector analyser and a quadrupole ion trap at flow rates of approximatly 1–5 μL/min (1×10^{-5} mol/L in H_2O/MeOH). Infrared spectra were recorded with a Nicolet 5PC FT-IR spectrophotometer using KBr pellets.

X-ray Crystallographic Study: Single crystals could be obtained from aqueous solutions by slow evaporation in air. A suitable crystal was fixed in a glass capillary and transferred onto the diffractometer (Table 3). The crystal was measured on a STOE IPDS diffractometer using graphite monochromated Mo-K_α radiation (λ = 71.073 pm). All calculations were performed using SIR92[17] and SHELXL-97.[18] All non-hydrogen atoms were refined anisotropically. The numerical absorption correction (X-RED V1.22; Stoe & Cie, 2001) was performed after optimizing the crystal shape using X-SHAPE V1.06 (Stoe & Cie, 1999).[19]

Table 3. Crystallographic data.[a]

Empirical formula	$C_4H_{26}N_{16}O_{13}Th$
Formula weight [g mol^{-1}]	738.4
Colour, habit	colourless, prism
Temperature [K]	293(2)
Crystal size [mm]	$0.2 \times 0.1 \times 0.1$
Crystal system	triclinic
Space group	$P\bar{1}$
a [pm]	1058.2(2)
b [pm]	1081.6(2)
c [pm]	1136.7(2)
α [°]	73.46(2)
β [°]	83.98(2)
γ [°]	66.01(2)
V [10^{-6} pm^3]	1139.4(4)
Z	2
Density (calcd.) [g cm^{-3}]	2.152
Absorption coefficient [mm^{-1}]	6.635
F(000)	712
Theta range [°]	3.19 to 28.08
Index range	$-13 < h < 13$ $-14 < k < 14$ $-14 < l < 14$
Reflections collected	9861
Independent reflections	5044
Observed reflections (2σ)	4662
R (int.)	0.0786
Data / restraints / parameters	4662 / 0 / 285
Goodness-of-fit F^2	1.126
R_1, wR_2 [$I > 4\sigma(I)$]	0.0581, 0.1619
R_1, wR_2 (all data)	0.0628, 0.1726
Largest difference peak / hole [e/pm^6]	3.8 / –4.5

[a] $R_1 = \Sigma \, ||F_o| - |F_c|| / \Sigma \, |F_o|$, $wR_2 = [\Sigma w(|F_o|^2 - |F_c|^2)^2 / \Sigma w(|F_o|^2)^2]^{1/2}$.

CCDC-692361 contains the supplementary crystallographic data for this paper. These data can be obtained free of charge from The Cambridge Crystallographic Data Centre via www.ccdc.cam.ac.uk/data_request/cif.

Computational Details

All calculations were carried out using the TURBOMOLE v. 5.10 system of programs[20] on an Intel® 2.4 GHz Quad-Core work-

station cluster. Generally, the atomic Th^{IV} subunits of rare gas-like $[Rn]7s^05f^06d^0$ configurations have been modeled within the relativistic *large-core* pseudopotential (PP) approximation:[21] In a somewhat simplified picture, Th^{IV} atomic orbitals with main quantum numbers $n \leq 5$ are replaced by potential functions fitted to accurate scalar-relativistic Wood–Boring all-electron reference data; the validity of this approach has recently been established.[22] For Th^{IV} a PP-compatible (5s6p4d2f1g)/[4s4p3d2f1g] Gaussian basis set with additional diffuse two s, one p, and one d functions[21] has been used. For H, C, and O the standard TZVP basis sets of Schäfer et al.[23] have been applied. Energy and molecular structure optimisations have been carried out on a Density Functional Theory (DFT) level with the TPSSh[24] exchance-correlation functional. TPSSh is a hybrid-type *meta*-GGA DF,[25] employing both exact exchange and kinetic energy densities, that has been found to perform successfully for both standard training sets and a collection of 4th period transition-metal systems.[26] As outlined in the Supporting Information, benchmark calculations on the experimentally known thorium(IV) croconate crystal structure $[Th(\eta^1\text{-}C_5O_5)_2(OH_2)_7]$[27] showed TPSSh to perform as good as, if not better than other GGA and hybrid-type DFs, and very similar to ab initio MP2 calculation schemes. As DFT exchange-correlation energy integrations are done numerically on element-specific grids in TURBOMOLE, and no thorium grid is implemented in v. 5.10, the lanthanum dynamic m3 grid was used. Total energies were converged below 10^{-7} a.u. Molecular structures, where converged, have been optimised to Cartesian gradient norms below 10^{-3} a.u.

Synthesis of Sodium 5,5′-Bitetrazolate: Manganese 5,5′-bitetrazolate[9] (40 g, 0.21 mol) and sodium carbonate (22.2 g, 0.21 mol) was suspended in water (500 mL) and heated at reflux for several hours. Manganese carbonate was filtered off and the water evaporated to obtain a slightly green solid. After several recrystallisations from water the solid became colourless and was dried in vacuo at 100 °C. Yield: 25.2 g (66%). ^{13}C NMR (100 MHz, D_2O, TMS): δ = 154.3 (s) ppm. MS (negative ESI): *m*/*z* (%): 137.17 (100) $[C_2HN_8]$, 159.14 (10) $[NaC_2N_8]$. IR (KBr): $\tilde{\nu}$ = 1631, 1458, 1345, 1327, 1307, 1182, 1148, 1072, 1048, 1016, 734, 586 (br) cm^{-1}. $C_{20}N_8Na_2$ (182.05): calcd. C 13.19, H 0.0, N 61.55; found C 12.94, H 0.0, N 59.21.

Synthesis of Thorium(IV) 5,5′-Bitetrazolate Hydrate: Th^{IV}nitrate hydrate (0.5 g, ca. 1 mmol) was dissolved in hot water (10 mL) and a solution of sodium 5,5′-bitetrazolate (0.6 g, 4 mmol) was added dropwise. After 24 h colourless crystals could be observed which were analysed by X-ray diffraction.

Supporting Information (see also the footnote on the first page of this article): $[Th(\eta^1\text{-}C_5O_5)_2(OH_2)_7]$ coordinates, interatomic distances and angles, and total energies calculated at HF, SVWN, BP86, BLYP, B3LYP, PBE0, TPSSh, and MP2 levels of theory; and $[(\mu\text{-}OH_2)_4Th_2(OH_2)_{12}]^{8+}$, $[(\mu\text{-}OH)_2Th_2(OH_2)_{14}]^{6+}$, $[Th(OH_2)_7]^{4+}$, $[Th(OH_2)_6OH{\cdot}OH_3]^{4+}$, $[Th(OH_2)_7OH]^{3+}$, H_2O, OH^-, and Th^{IV} coordinates and total energies calculated at the TPSSh level of theory.

Acknowledgments

We thank Dr. I. Pantenburg and I. Müller for the X-ray measurements. The financial support by the Deutsche Forschungsgemeinschaft (DFG) to J. W. is gratefully acknowledged.

[1] G. Seaborg, *Annu. Rev. Nucl. Sci.* **1968**, *18*, 53–152.
[2] W. H. Zachariasen, *Acta Crystallogr.* **1952**, *5*, 19–21.
[3] M. Haissinsky, *Nuclear Chemistry and its Applications*, New York, Addison-Wesley, **1964**, p. 206.
[4] G. Choppin, *J. Alloys Compd.* **1995**, *223*, 174–179.
[5] G. V. Ionova, *Russ. J. Coord. Chem.* **2001**, *4*, 237–248.
[6] K. C. Jantunen, B. L. Scott, J. L. Kiplinger, *J. Alloys Compd.* **2007**, *444*, 363–368.
[7] A. Yahia, L. Maron, *Organometallics* **2009**, *28*, 672–679.
[8] a) J. C. Green, M. de Simone, M. Coreno, A. Jones, H. M. I. Pritchard, G. S. McGrady, *Inorg. Chem.* **2005**, *44*, 7781–7793; b) J. C. Green, R. Shinomoto, N. Edelstein, *Inorg. Chem.* **1986**, *25*, 2718–2720.
[9] P. J. Eulgem, A. Klein, N. Maggiarosa, D. Naumann, R. W. H. Pohl, *Chem. Eur. J.* **2008**, *14*, 3727–3736 and references cited therein.
[10] a) E. Oliveri-Mandala, *Gazz. Chim. Ital.* **1920**, *50*, 256–261; b) W. Friedrich, D. B. P. 952811, **1956**; c) G. I. Koldobskii, V. A. Ostrovskii, B. V. Gidaspov, *Khim. Geterotsikl. Soedin.* **1980**, *7*, 867–879; *Chem. Abstr.*: 93237969.
[11] P. J. Steel, *J. Chem. Crystallogr.* **1996**, *26*, 399–402.
[12] J. H. Nelson, N. E. Takach, R. A. Henry, D. W. Moore, W. M. Tolles, G. A. Gray, *Magn. Reson. Chem.* **1986**, *24*, 984–994.
[13] R. E. Wilson, S. Skanthakumar, G. Sigmon, P. C. Burns, L. Soderholm, *Inorg. Chem.* **2007**, *46*, 2368–2372.
[14] R. E. Wilson, S. Skanthakumar, P. C. Burns, L. Soderholm, *Angew. Chem. Int. Ed.* **2007**, *46*, 8043–8045.
[15] W. Massa, *Kristallstrukturbestimmung*, 5 ed., Teubner, Stuttgart, **2007**; or: W. Massa, *Crystal Structure Determination*, 2 ed., Springer, Berlin, **2004**.
[16] R. D. Shannon, *Acta Crystallogr., Sect. A* **1976**, *32*, 751–767.
[17] *SIR*92, A program for automatic solution of crystal structures by direct methods: A. Altomare, G. Cascarano, C. Giacovazzo, A. Guagliardi, M. C. Burla, G. Polidori, M. J. Camalli, *J. Appl. Crystallogr.* **1994**, *27*, 435–436.
[18] *SHELXL-97*, A program for Crystal Structure Refinement: G. M. Sheldrick, University of Göttingen, **1997**.
[19] a) *STOE X-RED*, Data Reduction Program, Version 1.22/Windows, STOE & Cie, Darmstadt, **2001**; b) *STOE X-SHAPE*, Crystal Optimisation for Numerical Absorption Correction, Version 1.06/Windows, STOE & Cie, Darmstadt, **1999**.
[20] R. Ahlrichs, M. Bär, M. Häser, H. Korn, C. Kölmel, *Chem. Phys. Lett.* **1989**, *126*, 165–169.
[21] A. Moritz, X. Cao, M. Dolg, *Theor. Chem. Acc.* **2007**, *118*, 2763–2774.
[22] A. Moritz, M. Dolg, *Chem. Phys.* **2007**, *337*, 48–54.
[23] A. Schäfer, C. Huber, R. Ahlrichs, *J. Chem. Phys.* **1994**, *100*, 5829–5835.
[24] a) P. A. M. Dirac, *Proc. Camb. Philos. Soc.* **1930**, 376–385; b) J. C. Slater, *Phys. Rev.* **1951**, *81*, 385–390; c) J. P. Perdew, Y. Wang, *Phys. Rev. B* **1992**, *45*, 13244–13249; d) J. Tao, J. P. Perdew, V. N. Staroverov, G. E. Scuseria, *Phys. Rev. Lett.* **2003**, *91*, 146401-1-146401-4; e) V. N. Staroverov, G. E. Scuseria, J. Tao, J. P. Perdew, *J. Chem. Phys.* **2003**, *119*, 12129–12137.
[25] J. P. Perdew, K. Schmidt, *Density Functional Theory and Its Application to Materials*, (Eds.: V. van Doren, C. van Alsenoy, P. Geerlings), AIP PRESS, Melville, New York, **2001**.
[26] F. Furche, J. P. Perdew, *J. Chem. Phys.* **2006**, *124*, 004103-1-004103-1-27.
[27] C. Brouca-Cabarrecq, J.-C. Trombe, *Inorg. Chim. Acta* **1992**, *191*, 241−248.

Received: February 15, 2009
Published Online: May 7, 2009

